



King Saud University

Arabian Journal of Chemistry

www.ksu.edu.sa
www.sciencedirect.com



ORIGINAL ARTICLE

Acylhydrazide-based porous coordination polymers and reversible I₂ adsorption properties



Yan-Ning Wang ^{a,b}, Rong-Yan Wang ^a, Qing-Feng Yang ^c, Jie-Hui Yu ^{a,*}

^a College of Chemistry, State Key Laboratory of Inorganic Synthesis and Preparative Chemistry, Jilin University, Changchun, Jilin 130012, China

^b College of Chemistry and Chemical Engineering, Xinyang Normal University, Xinyang, Henan 464000, China

^c State Key Laboratory of High-efficiency Utilization of Coal and Green Chemical Engineering, and College of Chemistry and Chemical Engineering, Ningxia University, Yinchun 750021, China

Received 3 February 2018; accepted 3 July 2018

Available online 25 July 2018

KEYWORDS

Porous coordination polymers;
In situ;
Acylation;
I₂ adsorption;
Mutilcarboxylic acids

Abstract By employing the hydrothermal *in situ* acylation of organic acids with N₂H₄, three porous acylhydrazide-based Zn²⁺/Cd²⁺ coordination polymers as [M(L1)(H₂O)]·1.5H₂O (H₂L1 = benzimidazole-5,6-dihydrazide; M²⁺ = Zn²⁺ **1**, Cd²⁺ **2**) and [Zn(HL2)(H₂O)]·3H₂O (H₃L2 = 4,5-(di-3',4'-phthalhydrazide)) **3** were obtained. X-ray single-crystal diffraction analysis reveals that the frameworks of **1–3** can all be simplified into a (3_{metal node}·3_{ligand node})-connected net. However, since the ligands are different, they show the distinct structures: a C-tube-like structure for the isostructural **1** and **2**; a 10³ topology for **3**. The cif-checking reports indicate that the solvent accessible voids in the structures of **1–3** are 1055 Å³, 1282.4 Å³, and 978 Å³, respectively. It is noteworthy that **3** is the first example of triacylhydrazide-based coordination polymer. The investigation of the I₂-adsorption property for two Zn²⁺ compounds suggests that both can adsorb reversibly the I₂ molecule. The adsorption amount for **3** (100 mg adsorbing 22.0 mg I₂) is a bit higher than that for **1** (100 mg accommodating 15.6 mg I₂). However, the adsorption speed for **3** is much faster than that for **1**. About 5 s, the I₂ adsorption for **3** is close to saturation, while for **1**, it is about 20 days. This might be related to the number and the distribution for the uncoordinated N/O atoms on the side walls of the channels.

© 2018 Production and hosting by Elsevier B.V. on behalf of King Saud University. This is an open access article under the CC BY-NC-ND license (<http://creativecommons.org/licenses/by-nc-nd/4.0/>).

1. Introduction

* Corresponding author.

E-mail address: jhyu@jlu.edu.cn (J.-H. Yu).

Peer review under responsibility of King Saud University.



Production and hosting by Elsevier

Much attention has been paid to the design and synthesis of novel porous coordination polymer materials due to their structural diversity (Fang et al., 2015a, 2015b; Zhang et al., 2015a, 2015b, 2015c, 2015d; Herzberger et al., 2016), and the potential applications in adsorption (Levine et al., 2016a, 2016b, 2016c, 2016d; Lin et al., 2017a, 2017b; Nandi et al., 2017a, 2017b; Ahmed and Rothenberger, 2016a, 2016b;

Garai and Biradha, 2017), storage (Gygi et al., 2016a, 2016b; Gao et al., 2017a, 2017b; Al-Maythalony et al., 2015a, 2015b; Hu et al., 2017a, 2017b; Du et al., 2015), separation (Gelfand et al., 2016a, 2016b; Li et al., 2009a, 2009b; Xue et al., 2015a, 2015b; Zhang et al., 2016a, 2016b, 2016c, 2016d, 2016e, 2016f, 2016g), purification (Sikdar et al., 2016a, 2016b; Yuan et al., 2016a, 2016b; Chaemchuen et al., 2015), ion exchange (Li et al., 2015a, 2015b; Zhao et al., 2015a, 2015b; Cao et al., 2015a, 2015b, 2015c; Xu et al., 2015), sensing (Chen and Jiang, 2016a, 2016b; Ye et al., 2015a, 2015b; Cui et al., 2015a, 2015b, 2015c, 2015d; Luo et al., 2015), and medicine delivery (Levine et al., 2016a, 2016b, 2016c, 2016d; Wang et al., 2016a, 2016b, 2016c, 2016d, 2016e, 2016f, 2016g, 2016h, 2016i, 2016j). For example, (i) the porous coordination polymer materials, in particular the multicarboxylate-based porous coordination polymer materials, have been confirmed to be able to adsorb various gases, which can be applied in the energy storage (H_2 adsorption) (Lucier et al., 2016a, 2016b; Rosnes et al., 2015a, 2015b; Blanita et al., 2015) and the air purification (CO_2 adsorption) (Gao et al., 2016a, 2016b, 2016c, 2016d; Ugale et al., 2016a, 2016b; Hong et al., 2015). And, some porous coordination polymers with the special porous structures can selectively adsorb some substance. This kind of porous material can be applied in the substance separation and purification; (Ma et al., 2016a, 2016b, 2017a, 2017b; Zhang et al., 2016a, 2016b, 2016c, 2016d, 2016e, 2016f; 2016g; Jiao et al., 2016) (ii) for some organically templated porous coordination polymer materials, the templating agent as $CH_3NH_2^+$ has been verified to be exchanged by the cationic dye molecule, which can be applied in the removal of the dye pollutants in the water; (Xie et al., 2016a, 2016b; Luo et al., 2017a, 2017b; Zhang et al., 2015a, 2015b, 2015c, 2015d; Yao et al., 2017) (iii) after encapsulating some substance in the pore, some porous coordination polymer materials show a new property, or a large change for the property maybe occurs. This not only provides a new approach for the material fabrication, these porous materials can also act as the chemosensors to detect these substances (Cui et al., 2016a, 2016b; Desai et al., 2015a, 2015b; Yi et al., 2016a, 2016b; Wang et al., 2016a, 2016b, 2016c, 2016d, 2016e, 2016f, 2016g, 2016h, 2016i, 2016j; Xie et al., 2017). Recently, the researchers find that some porous coordination polymer materials can reversibly adsorb the I_2 molecule (Yao et al., 2016a, 2016b; Wang et al., 2016a, 2016b, 2016c, 2016d, 2016e, 2016f, 2016g, 2016h, 2016i, 2016j; Zhu et al., 2016). This means that in the future, maybe the porous coordination polymer materials can displace the traditional Ag-containing zeolite materials (expensive, low efficient) to serve as the I_2 adsorbing agents. Moreover, the researchers also find that the I_2 -encapsulated porous coordination polymer materials can catalyze some organic reactions, and the I_2 -encapsulated molecule plays a key role in the reactions (Brunet et al., 2017).

The same as the metal center and the guest molecule, the ligand plays a crucial role in controlling the network structure and the porous size for the material. So far, a number of bridging-type organic ligands including the organic acids (Lee et al., 2016a, 2016b; Zanchetta et al., 2015a, 2015b; Gao et al., 2016a, 2016b, 2016c, 2016d; Li et al., 2016a, 2016b, 2016c, 2016d; Gabriel et al., 2015a, 2015b; Maiti et al., 2016a, 2016b; Li et al., 2016a, 2016b, 2016c, 2016d; Wang et al., 2015a, 2015b, 2015c), organic bases (Krause

et al., 2016a, 2016b; Shi et al., 2015a, 2015b; Manna et al., 2015a, 2015b; Zhang et al., 2016a, 2016b, 2016c, 2016d, 2016e, 2016f, 2016g; Tang et al., 2016), and the other N/O-donor molecules (Chen et al., 2015a, 2015b, 2015c, 2015d; Zhang et al., 2016a, 2016b, 2016c, 2016d, 2016e, 2016f, 2016g; Huang et al., 2015a, 2015b; Karmakar et al., 2016) have been employed in the construction of novel porous coordination polymer materials. However, the acylhydrazide molecules are seldom considered (Whitcomb and Rajeswaran, 2006a, 2006b; Morzyk-Ociepa, 2007a, 2007b, 2007c, 2007d; Zhang et al., 2008a, 2008b; Ahmad et al., 2014a, 2014b, 2014c). In the past, we have employed pyridine-3,4-dicarboxylhydrazide (HL3) and 4-carboxylphthalhydrazide (H₂L4) (see Scheme S1) to construct several porous coordination polymer materials (Yu et al., 2009a, 2009b; Wang et al., 2014a, 2014b, 2014c, 2014d, 2014e, 2014f, 2014g). But since the distance between the acylhydrazine group and the other donor atoms is short, only the small pore is observed in the network structure. In order to enlarge the distance between the acylhydrazine group and the other donor atoms, the acylhydrazide molecules 4-(3-carboxylphenoxy)phthalhydrazide (H₂L5) and 4-(4-carboxylphenoxy)phthalhydrazide (H₂L6) were selected to act as the ligand precursors (see Scheme S1). However, not only the expected large pore is not observed, but also just two chained compounds are formed (Wang et al., 2014a, 2014b, 2014c, 2014d, 2014e, 2014f, 2014g). This might be due to the flexibility of these two acylhydrazide molecules. In this article, we design two new acylhydrazide molecules H₂L1 (benzimidazole-5,6-dihydrazide) and H₃L2 (4,5-(di-(3',4'-phth alhydrazide))). Note that (i) in H₂L1 and H₃L2, the distance between the acylhydrazine group and the other donor atoms is long; (ii) two acylhydrazide molecules possess the better rigidity. As expected, three acylhydrazide-based porous coordination polymers as [M(L1)(H₂O)]·1.5H₂O ($M^{2+} = Zn^{2+}$ **1**, Cd^{2+} **2**), and [Zn(HL2)(H₂O)]·3H₂O **3** were obtained. The acylhydrazide molecules derive from the hydrothermal *in situ* acylation of organic acids with N_2H_4 (see Scheme 1). The I_2 -adsorption properties for two Zn^{2+} compounds are investigated.

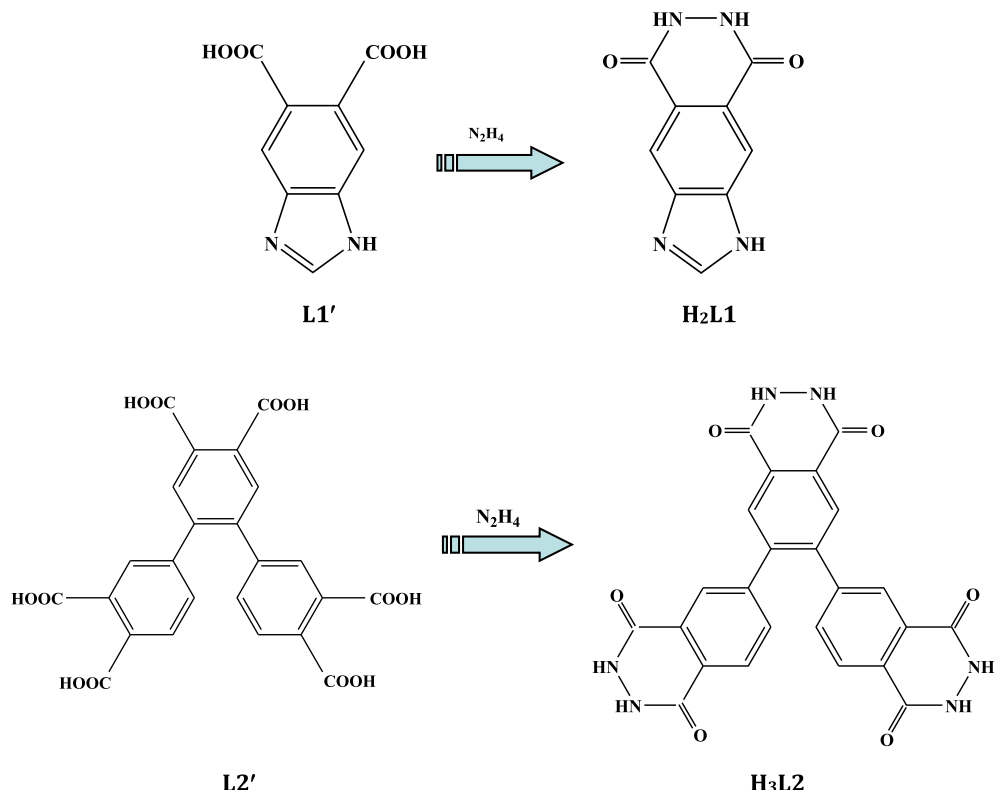
2. Experimental

2.1. Materials and physical measurement

All chemicals are of reagent grade quality, obtained from commercial sources without further purification. Elemental analysis (C, H and N) was performed on a Perkin-Elmer 2400LS II elemental analyzer. Infrared (IR) spectrum was recorded on a Perkin Elmer Spectrum *I* spectrophotometer in 4000–400 cm^{-1} region using a powdered sample on a KBr plate. Powder X-ray diffraction (XRD) data were collected on a Rigaku/max-2550 diffractometer with Cu-*K* radiation ($\lambda = 1.5418 \text{ \AA}$). Thermogravimetric (TG) behavior was investigated on a Perkin-Elmer TGA-7 instrument with a heating rate of 10 $^\circ\text{C min}^{-1}$ in air. Ultraviolet-visible (UV-Vis) spectrum was obtained on a Rigaku-UV-3100 spectrophotometer.

2.2. Synthesis of **1–3**

[Zn(L1)(H₂O)]·1.5H₂O 1. The yellow column crystals of **1** were obtained from a simple hydrothermal self-assembly of Zn



Scheme 1 In situ acylation of organic acids with N_2H_4 ($\text{L}1' = \text{benzimidazole-5,6-dicarboxylic acid}$; $\text{L}2' = [\text{1},\text{1}',\text{2}',\text{1}''\text{-terphenyl}-\text{3},\text{3}'',\text{4},\text{4}',\text{4}'',\text{5}'\text{-hexacarboxylic acid}]$).

$(\text{CH}_3\text{COO})_2\cdot 2\text{H}_2\text{O}$ (11 mg, 0.05 mmol), $\text{L}1'$ (10 mg, 0.05 mmol), and $\text{N}_2\text{H}_4\cdot \text{H}_2\text{O}$ (0.2 mL) in a 15 mL aqueous solution (pH = 5 adjusted by $\text{H}_2(\text{C}_2\text{O}_4)$ ($\text{C}_2\text{O}_4^{2-} = \text{oxalate}$)) at 170 °C for 4 days. Yield: *ca.* 20% based on Zn(II). Anal. Calcd $\text{C}_{9}\text{H}_9\text{N}_4\text{O}_4\text{Zn}$ **1**: C 34.80, H 2.92, N 18.04%. Found: C 35.36, H 2.82, N 18.10%. IR (cm^{-1}): 1628 s, 1572 s, 1503 s, 1413 s, 1302 s, 1230 s, 1180 m, 1058 m, 897 w, 859 m, 645 w, 538 w.

[Cd(L1)(H₂O)]·1.5H₂O **2**. The yellow block crystals of **2** were obtained from a simple hydrothermal self-assembly of $\text{Cd}(\text{CH}_3\text{COO})_2\cdot 2\text{H}_2\text{O}$ (14 mg, 0.05 mmol), $\text{L}1'$ (10 mg, 0.05 mmol), and $\text{N}_2\text{H}_4\cdot \text{H}_2\text{O}$ (0.2 mL) in a 15 mL aqueous solution (pH = 7 adjusted by N_2H_4) at 170 °C for 4 days. Yield: *ca.* 25% based on Cd(II). Anal. Calcd $\text{C}_{9}\text{H}_9\text{N}_4\text{O}_4\text{.5Cd}$ **2**: C 30.23, H 2.54, N 15.67%. Found: C 29.53, H 2.80, N 15.48%. IR (cm^{-1}): 1626 s, 1567 s, 1489 s, 1468 s, 1435 m, 1358 s, 1302 s, 1231 m, 1183 m, 1055 m, 854 m, 631 m.

[Zn(HL2)(H₂O)]·3H₂O **3**. The yellow block crystals of **3** were obtained from a simple hydrothermal self-assembly of $\text{Zn}(\text{CH}_3\text{COO})_2\cdot 2\text{H}_2\text{O}$ (9 mg, 0.04 mmol), $\text{L}2'$ (10 mg, 0.02 mmol), and $\text{N}_2\text{H}_4\cdot \text{H}_2\text{O}$ (0.1 mL) in a 10 mL aqueous solution (pH = 6 adjusted by $\text{H}_2(\text{C}_2\text{O}_4)$) at 170 °C for 4 days. Yield: *ca.* 20% based on Zn(II). Anal. Calcd $\text{C}_{24}\text{H}_{20}\text{N}_6\text{O}_{10}\text{Zn}$ **3**: C 46.65, H 3.26, N 13.61%. Found: C 46.43, H 3.80, N 13.56%. IR (cm^{-1}): 1642 m, 1570 m, 1513 s, 1384 s, 1251 w, 1217 m, 1079 m, 910 w, 809 w, 724 m, 675 m, 571 m.

2.3. X-ray crystallography

The data were collected with Mo- $K\alpha$ radiation ($\lambda = 0.71073 \text{ \AA}$) on a Siemens SMART CCD diffractometer for **1–3**. With

SHELXTL program, the structures of all were solved using direct methods (Sheldrick, 2008). The non-hydrogen atoms were assigned anisotropic displacement parameters in the refinement, and the other hydrogen atoms were treated using a riding model. The hydrogen atoms on the coordinated water molecules in the title compounds were not located. The guest water molecules in **1–3** suffer severe disorder, so the PLATON program is employed to solve this problem. The structures were then refined on F^2 using SHELXL-97 (Sheldrick, 2008). The CCDC numbers are 1458076–1458078 for **1–3**, respectively (see Table 1).

3. Results and discussion

3.1. Synthetic analysis

All of the title compounds were obtained under the hydrothermal conditions. The simple self-assemblies of $\text{Zn}^{2+}/\text{Cd}^{2+}$, organic acids and N_2H_4 created the title compounds **1–3**. The acylhydrazide molecules in **1–3** originated from the hydrothermal *in situ* acylation of organic acids with N_2H_4 . The single-crystal growth and the purity are strictly controlled by the pH level of the reactive system: 5 for **1**, 7 for **2**, and 6 for **3**. $\text{H}_2\text{C}_2\text{O}_4$ and N_2H_4 were generally used to adjust the pH value of the reactive system. All of the reactions were carried out at 170 °C. Maybe only at the higher temperature as 170 °C, the acylation of organic acids with N_2H_4 could occur. In the reactions, N_2H_4 is largely excessive in order to ensure the carboxyls to be thoroughly acylated. For the reactions of **1** and **2**, once Mn^{2+} instead of Zn^{2+} or Cd^{2+} is used, a dinu-

Table 1 Crystal data of **1–3**.

	1	2	3
Formula	C ₉ H ₉ N ₄ O _{4.5} Zn	C ₉ H ₉ N ₄ O _{4.5} Cd	C ₂₄ H ₂₀ N ₆ O ₁₀ Zn
<i>M</i>	310.57	357.61	617.83
<i>T</i> (K)	293(2)	293(2)	293(2)
Crystal system	Rhombohedral	Rhombohedral	Monoclinic
Space group	<i>R</i> -3	<i>R</i> -3	<i>C</i> 2/c
<i>a</i> (Å)	24.192(3)	25.002(3)	11.001(2)
<i>b</i> (Å)	24.192(3)	25.002(3)	25.507(5)
<i>c</i> (Å)	9.6003(19)	9.968(2)	17.270(4)
α (°)	90	90	90
β (°)	90	90	93.56(3)
γ (°)	120	120	90
<i>V</i> (Å ³)	4865.7(14)	5396.2(14)	4836.6(17)
<i>Z</i>	18	18	8
<i>D</i> _c (g cm ⁻³)	1.742	1.831	1.549
μ (mm ⁻¹)	2.273	1.822	1.073
Reflections collected	15,879	17,056	23,380
Unique reflections	2481	2753	5512
<i>R</i> _{int}	0.0392	0.0329	0.0755
Gof	1.135	1.175	1.088
<i>R</i> ₁ , <i>I</i> > 2σ(<i>I</i>)	0.0475	0.0502	0.1205
<i>wR</i> ₂ , all data	0.1527	0.1700	0.3645

clear Mn²⁺ complex [Mn₂(HL1)₂(C₂O₄)(H₂O)₆]·2H₂O was obtained (Wang et al., 2016a, 2016b, 2016c, 2016d, 2016e, 2016f, 2016g, 2016h, 2016i, 2016j). For the reaction of **3**, once Ni²⁺ instead of Zn²⁺ was used, the 3-D complex [Ni(C₂O₄)(N₂H₄)]·H₂O was obtained (Wang et al., 2017). Note that this compound is constructed by a mixed ligand of N₂H₄ and C₂O₄²⁻, and H₃L2 did not appear in the final backbone. While once Pb²⁺ instead of Zn²⁺ was used, an isostructural Pb²⁺ complex to **1** and **2** was obtained. Due to severe disorder for the Pb²⁺ center, the crystal data of this complex did not pass the cif-checking examination.

3.2. Structural description

[M(L1)(H₂O)]·1.5H₂O (**M**²⁺ = Zn²⁺ **1**, Cd²⁺ **2**). X-ray single-crystal diffraction analysis reveals that **1** and **2** are isostructural to each other. So only the structure of **1** as the representative will be described here. **1** is a 1-D tubed Zn²⁺ coordination polymer constructed from the L1²⁻ molecule. It crystallizes in the space group *R*-3, and the asymmetric unit is found to be composed of one Zn²⁺ ion (Zn1), one L1²⁻ molecule, and one coordinated water molecule (Ow1). The lattice water molecules are confirmed by the CHN and TG analyses. As shown in Fig. 1a, Zn1 with a tetrahedral geometry is coordinated by one hydroxylimino N atom (N1), two imidazo N atoms (N3a, N4b) and one water molecule (Ow1). The Zn1-N range and the Zn1-Ow distance are 1.979(3)–2.014(3) Å and 2.043(3) Å, respectively. For the ligand, three information can be obtained, based on the crystal data: (i) L1²⁻ adopts a triple-bridged coordination mode with the imidazo N atoms and the hydroxylimino N atom as the donors (see Fig. 1b); (ii) the acylhydrazine moiety exists in a keto-hydroxyl form, which is revealed by two different C-O distances (C7-O1 = 1.271(5) Å, C8-O2 = 1.258(5) Å). This also implies that the isomerization for one acylamino group has occurred (see Scheme S2); (iii) L1 has a -2 change: the hydro-

xyl group deprotonates; the imidazo N atom deprotonates. As exhibited in Fig. 1c, the μ₃-mode L1²⁺ molecules extend the tetrahedral Zn²⁺ centers into a 1-D endless chain, running down the *c*-axial direction. The chain possesses a tube-like structure with a larger circular window (diameter: ca. 11 Å), as shown in Fig. 1d. The topological method can be employed to better understand this tube structure. As displayed in Fig. 1e, the Zn²⁺ center and the L1²⁻ molecule can both be simplified into the 3-connected nodes, so the topology of this chain shows a C-tube-like structure. Fig. S1 is the projection plot of **1** in the (0 0 1) direction. Via the π···π interactions between the L2 molecules (separation: 3.37 Å), all of the 1-D tubes stack together into a 3-D supramolecular network. Even though the lattice water molecule is not located, they should occupy the space within the tube. The cif-checking report indicates that the solvent accessible void is 1055 Å³ in the structure of **1** (1282.4 Å³ in the structure of **2**).

[Zn(HL2)(H₂O)]·3H₂O **3**. **3** is a 3-D Zn²⁺ coordination polymer constructed from the HL2²⁻ molecule. It crystallizes in the space group *C*2/c, and the asymmetric unit is found to be composed of one Zn²⁺ ion (Zn1), one HL2²⁻ molecule, and one coordinated water molecule (Ow1). The lattice water molecules are determined by the CHN and TG analyses. As shown in Fig. 2a, Zn1 is in a tetrahedral site, surrounded by two acylamino N atoms (N1, N6b), one hydroxylimino N atom (N3a), and one water molecule (Ow1; Zn1-Ow1 = 2.016(10) Å). The Zn1-N range is 2.040(7)–2.059(7) Å. According to the crystal data, three information about HL2²⁻ can be gotten: (i) HL2²⁻ adopts a μ₃ coordination mode with N1, N3, and N6 as the donor atoms. Since three N atoms come from three different acylhydrazine moieties, HL2²⁻ acts as a tripodal ligand; (ii) two acylhydrazine moieties exist in a diketo form (C7-O1 = 1.247(12) Å, C8-O2 = 1.246(11) Å; C24-O6 = 1.253(10) Å, C23-O5 = 1.253(10) Å), whereas the third exists in a keto-hydroxyl form (C15-O3 = 1.266(11) Å, C16-O4 = 1.252(11) Å); (iii) HL2²⁻ shows a -2 oxidation state:

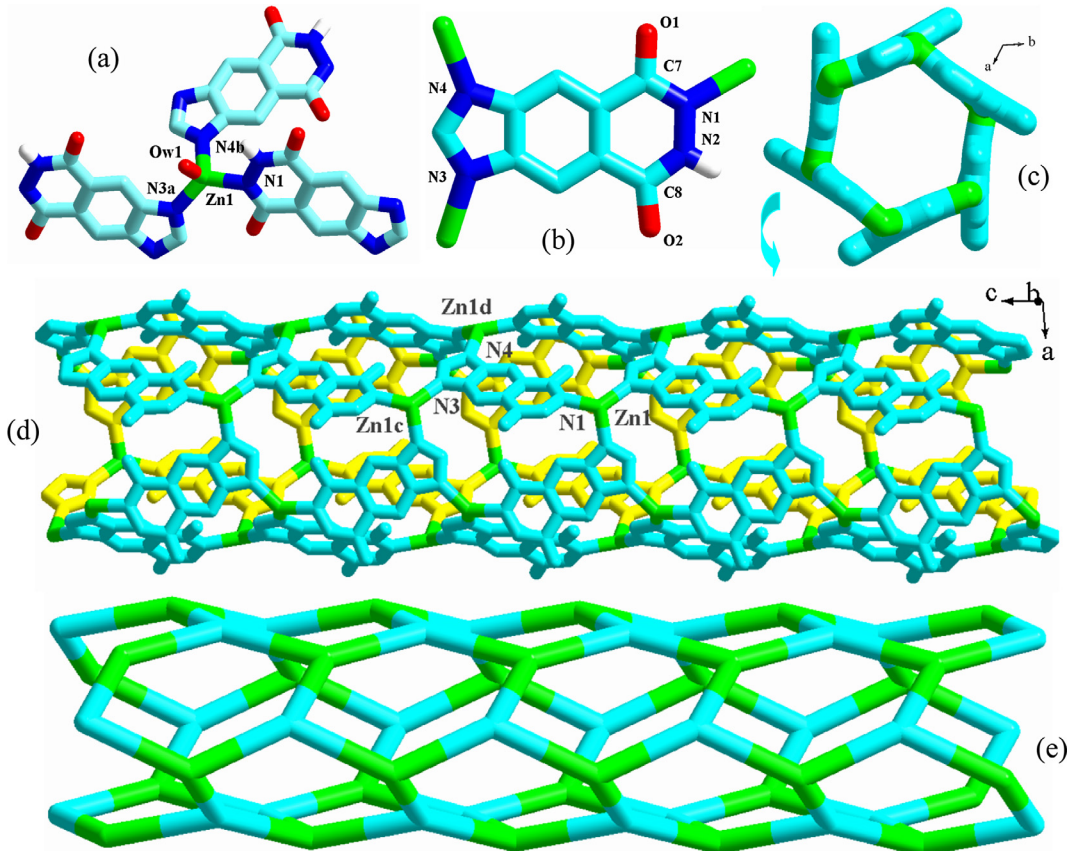


Fig. 1 Coordination environment around Zn1 (a), coordination mode of L^{2-} (b), 1-D tube (c, d) and its topology (e) for **1** (a: $x, y, z - 1$; b: $y, -x + y, -z - 1$; c: $x, y, z + 1$; d: $x - y, x, -z - 1$).

the protons on N1 and N6 are lost; the proton on O1 is not lost (see Scheme S2). Fig. 2c is the projection plot of **1** in (1 0 0) direction. The tripodal HL^{2-} molecules propagate the Zn (II) centers into a 3-D network. Only in this projection direction, the 1-D channels with the larger windows, extending along the *a*-axial direction, are observed. Based on the topological viewpoint, both the Zn^{2+} center and the HL^{2-} molecule can be viewed as a 3-connected node, so the 3-D network of **3** has a (3,3)-connected 10^3 topology (see Fig. 2d). As shown in Fig. S2, the 2-fold interpenetration phenomenon occurs in **3**. Even though the space for the channel turns small, the channel still exists. The cif-checking report for **3** indicates that the solvent accessible void in the structure of **3** is 978 \AA^3 . The lattice water molecules should occupy the space of these voids.

3.3. Structural discussion

The isostructural compounds **1** and **2** are the second examples of L^{2-} -based coordination polymers. The first example is a dinuclear Mn^{2+} complex (Sheldrick, 2008). **3** is the first example of triacylhydrazide-based coordination polymer. **1–3** all possess the porous structures. So far, the acylhydrazide-based porous coordination polymers are seldom reported. In **1–3**, the formation of the pores should be related to the following several factors: (i) the configuration of the ligand node. In L^{2-} and HL^{2-} , there exist so many potential donor atoms (6 in L^{2-} , 12 in HL^{2-}). But whether for L^{2-} or for

HL^{2-} in **1–3**, only three N atoms act as the donor atoms. The most important is that both can be simplified into a tripodal 3-connected node. It is said that this type of ligand node tends to form a porous network with the metal center; (Yu et al., 2016a, 2016b; Wang et al., 2016a, 2016b, 2016c, 2016d, 2016e, 2016f, 2016g, 2016h, 2016i, 2016j; Chen et al., 2015a, 2015b, 2015c, 2015d; Huang et al., 2016) (ii) the tetrahedral configuration for the metal center. The tetrahedral metal center is generally simplified into a 4-/3-connected node with a triangular pyramidal/tetrahedral configuration. This type of metal node tends to form a porous network with the ligand node (Wang et al., 2016a, 2016b, 2016c, 2016d, 2016e, 2016f, 2016g, 2016h, 2016i, 2016j; Fan et al., 2015a, 2015b; Parshamoni et al., 2016). In **1–3**, the metal centers all exhibit a tetrahedral configuration. In the unreported porous coordination polymer $[\text{Pb}(\text{HL}2)(\text{H}_2\text{O})] \cdot x\text{H}_2\text{O}$, the Pb^{2+} center is also in a tetrahedral site. While in the reported L^{2-} -based Mn^{2+} complex, the Mn^{2+} center adopts an octahedral geometrical configuration, so only a dinuclear structure is formed; (Sheldrick, 2008) (iii) the long distance between the acylhydrazine group and the other donor atoms. As displayed in Fig. 1c and 2c, the size of the pore is determined by the distance between the acylhydrazine group and the other donor atoms. The longer this distance is, the larger the pore is (interpenetration is temporarily ignored). In the reported compounds $[\text{Pb}(\text{L}3)_2]$ (Yu et al., 2009a, 2009b) and $[\text{Ba}_2(\text{L}4)_2(\text{H}_2\text{O})_2]$, (Wang et al., 2014a, 2014b, 2014c, 2014d,

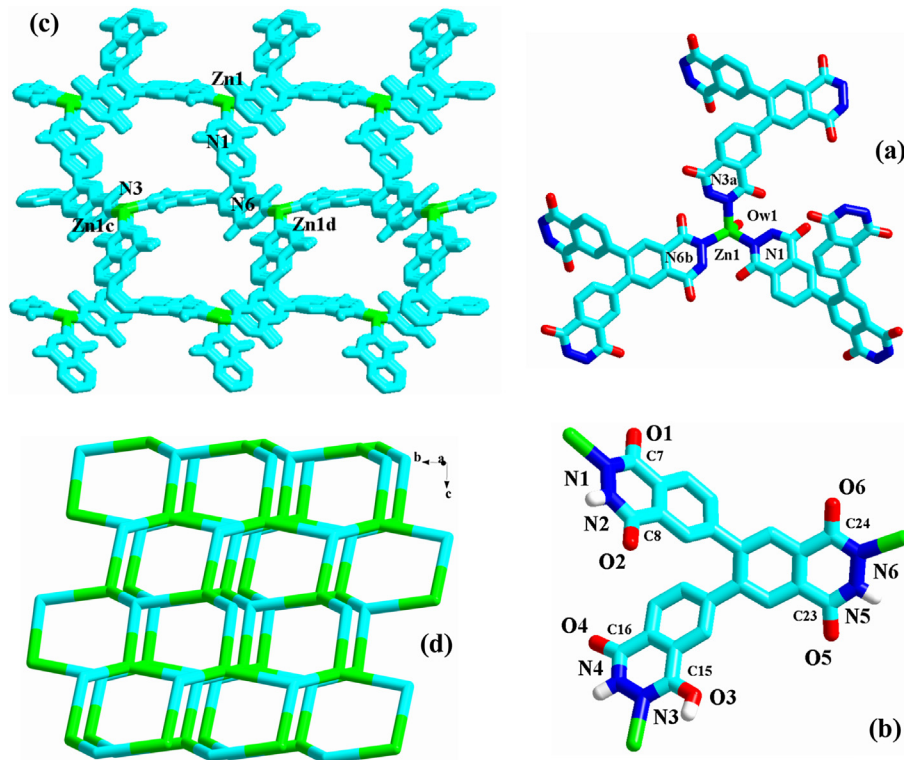


Fig. 2 Coordination environment around Zn1 (a), coordination mode of HL₂²⁻ (b), 3-D network (c) and its topology (d) for **3** (a: $x, y, z + 1$; b: $y, -x + y, -z + 1$; c: $x - y, x, -z + 1$; d: $x, y, z - 1$).

2014e, 2014f, 2014g) since the distance between the acylhydrazine group and the other donor atoms is short (see Scheme S1), only the small pore are observed in the 3-D network of these two complexes; (iii) the rigidity of the ligand. For H₂L5 and H₂L6 (see Scheme S1), the distance between the acylhydrazine group and the carboxyl group is not short, but not only the expected large pore is not observed, but also just two chained compounds [Zn(L5)(H₂O)] and [Zn(L6)] are formed (Wang et al., 2014a, 2014b, 2014c, 2014d, 2014e, 2014f, 2014g). This might be related to the flexibility of these two acylhydrazide molecules. Moreover, for the title three compounds, the network structures for them can all be simplified into a (3,3)-connected net. However, they exhibit the different topological structures: a C-tube-like topology for **1–2**; a 10³ topology for **3**. This should be related to the ligand including its category, its size and the position of the donor atom.

3.4. Characterization

3.4.1. TG analysis

Based on the elemental analysis, the number of the lattice water molecule in the asymmetric units of **1–3** can be preliminarily confirmed: 1.5 lattice water molecules in **1–2**; 3 lattice water molecules in **3**. In order to further validate the correctness of this conclusion, the TG behaviors of **1–3** in a temperature range of 20–800 °C in an air atmosphere were investigated. As shown in Fig. 3, both **1** and **2** underwent three steps of weight loss, corresponding to the sequential removals of the lattice water molecule, coordinated water molecule, and the acylhydrazide molecule. In the third step, the metal

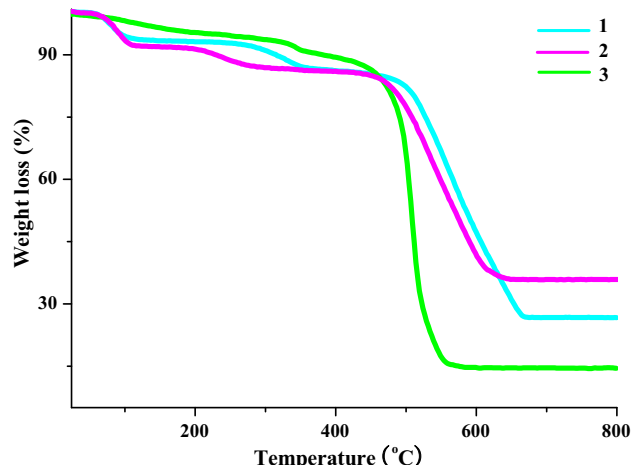


Fig. 3 TG curve of **1–3**.

center will combine with the O₂ molecule to form the metal oxide. The calculated weight-loss values (8.7%, 5.8%, 59.3% for **1**; 7.6%, 5.0%, 51.5% for **2**) are well comparable with those observed (ca. 7.0%, ca. 6.0%, ca. 60.0% for **1**; ca. 8.0%, ca. 6.0%, ca. 50.0% for **2**), suggesting that the confirmed number of the lattice water molecule in **1–2** is correct. For the TG curve of **3**, after losing the lattice or coordinated water molecule, no obvious platform is observed. However, the residue content (ca. 14.0%) is well comparable with that calculated (13.1%), implying that the confirmed number of the lattice water molecule in **3** is also correct.

3.4.2. Powder XRD patterns

In order to confirm the purity of the as-synthesized samples, the powder XRD analysis of **1–3** were performed. As exhibited in Figs. 4 and S3, the experimental powder XRD pattern for each compound is in accord with the simulated one generated on the basis of structural data, suggesting that the as-synthesized product is pure phase.

3.4.3. IR spectrum analysis

The IR characteristic peak of the acylamino group generally appears within the wavelength range of 1670–1625 cm⁻¹, while the IR characteristic peak of the —COOH group is either larger than 1670 cm⁻¹, or smaller than 1625 cm⁻¹ (Wang et al., 2013a, 2013b, 2014a, 2014b, 2014c, 2014d, 2014e, 2014f, 2014g). Based on this, we can quickly judge whether the acylation of organic acid with N₂H₄ has occurred. In the IR spectra of **1–3**, the appearance of the characteristic peak of the acylamino group (1628 cm⁻¹ for **1**, 1626 cm⁻¹ for **2**, 1642 cm⁻¹ for **3**) suggests that the organic acids have interacted with N₂H₄ into the acylhydrazide molecules, which is in agree-

ment with the results obtained from the crystal data (see Fig. 5).

3.5. Reversible I₂ adsorption property

Some porous coordination polymers have demonstrated the better reversible I₂ adsorption properties (Lin et al., 2016a, 2016b; Du et al., 2016a, 2016b; Zhao et al., 2017). This has been thought to be related to the porous size and the distribution of the N, O and X atoms on the porous side walls. The title compounds also possess the porous structures. Meanwhile, on the porous side walls, there exist many N and O atoms. In particular, most of them are uncoordinated. These atoms will directly affect the adsorption property of the material on the I₂ molecule via the weak N/O···I and N/O-H···I interactions. Based the consideration of these two factors above, we investigated the reversible I₂ adsorption properties of the title two Zn²⁺ compounds.

In order to investigate their I₂ adsorption properties, a 0.1 mol · dm⁻³ I₂ hexane solution (3 mL) was prepared, and then 100 mg powder sample for **1** or **3** was dispersed in this solution. Fig. 6 shows the time vs solution color images for **1** and **3**. As time goes on, the solution color for both turns light, suggesting that both **1** and **3** can adsorb the I₂ molecule. However, this does not mean that the adsorption must originate from the pore structure. Maybe it is a surface adsorption. So the sample was filtrated, and then washed with cyclohexane until the washing liquor shows a colorlessness, implying that I₂ on the surface has been completely removed. Fig. 6 also shows the time vs sample color images for **1** and **3**. The sample color gradually becomes dark, indicating that the pore for **1** and **3** can encapsulate the I₂ molecule to form **1@I₂** and **3@I₂**. The powder XRD analysis for **1@I₂** and **3@I₂** are carried out. As shown in Fig. 7, the powder XRD pattern does not alter, suggesting that the host architecture for each is still maintained after the I₂ uptake. Based on Fig. 6, we also know that for **3**, only about 5 s, the solution color does not change any more, indicating that the adsorption for **3** has been close to the saturation. This means that **3** can quickly adsorb the I₂ molecule. While for **1**, it is about 20 d.

In order to estimate the adsorption ability of the title two Zn²⁺ compounds, the TG behaviors for **1@I₂** and **3@I₂** were investigated. As displayed in Fig. 8, the initial weight loss (*ca.* 20% for **1@I₂**; *ca.* 22% for **3@I₂**) should be attributed to the removal of the I₂ molecule and the coordinated H₂O molecule. Based on this, two conclusions can be obtained through a simple calculation: (i) the real composition for **1@I₂** is [Zn(L₁) (H₂O)]·0.19I₂, while for **3@I₂**, it is [Zn(HL₂)(H₂O)]·0.54I₂; (ii) every 100 mg **1** can accommodate *ca.* 15.6 mg I₂, whereas every 100 mg **3** can accommodate *ca.* 22.0 mg I₂. Obviously, the I₂ adsorption capacity for **3** is slightly stronger than that for **1**.

In order to investigate whether the I₂ sorption process for **1** and **3** is reversible, 30 mg I₂-captured sample for **1** or **3** was immersed in a 3 mL ethanol solution. As exhibited in Fig. 9, the color of the ethanol solution gradually changes from the colorlessness, through the yellow, to the final orange. This suggests that in the ethanol solvent, the encapsulated I₂ molecule in **1** and **3** can be easily released from the pore. This also suggests that the I₂ adsorption processes for **1** and **3** are both reversible. The powder XRD patterns of the I₂-released

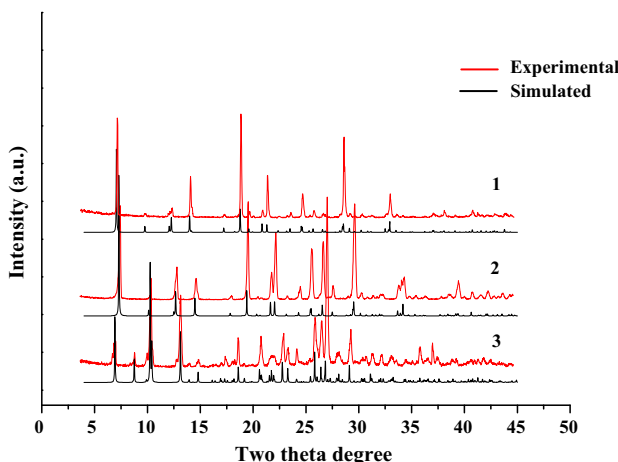


Fig. 4 Simulated (black) and experimental (red) powder XRD patterns of **1–3**.

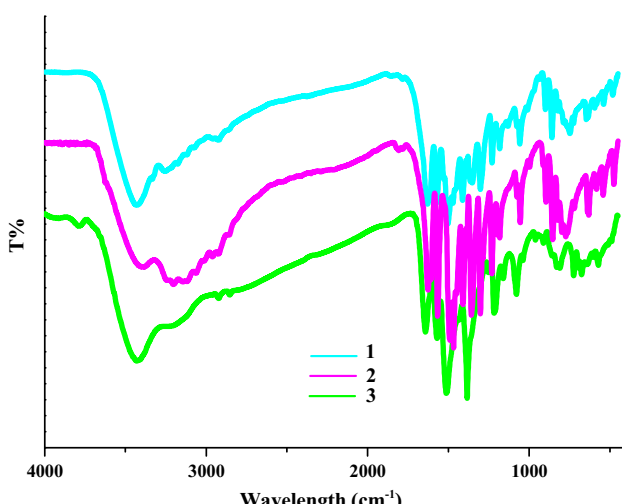


Fig. 5 IR spectra of **1–3**.

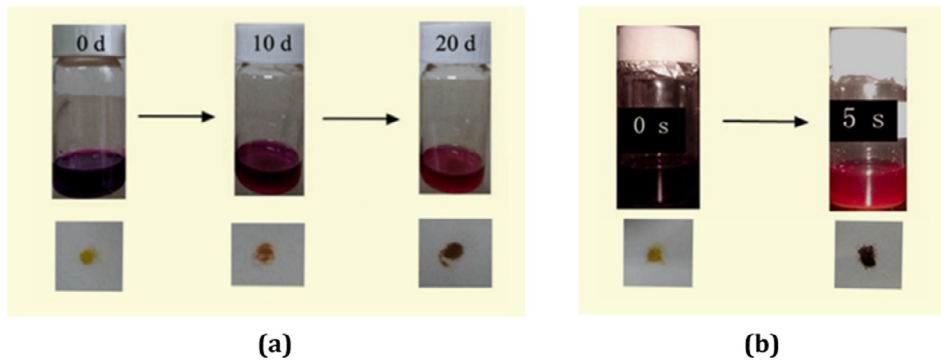


Fig. 6 Time *vs* solution color images, and time *vs* sample color images for **1** (a) and **3** (b).

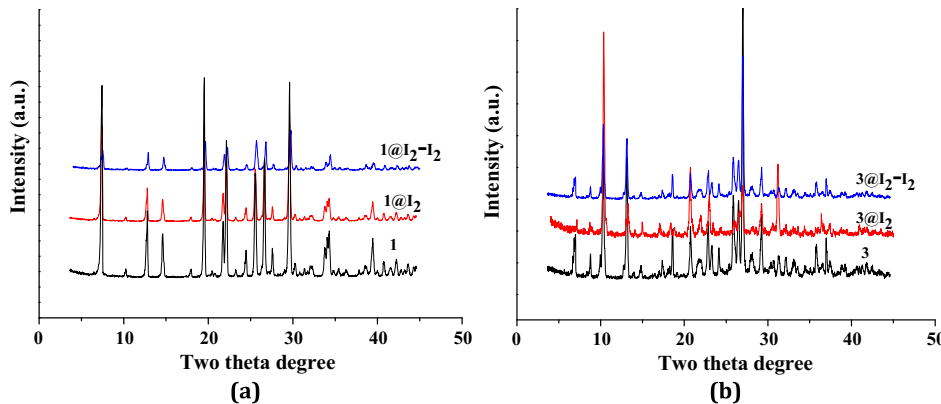


Fig. 7 Powder XRD patterns of I₂-absorbed sample, I₂-released sample, and corresponding title compound for **1** (a) and **3** (b).

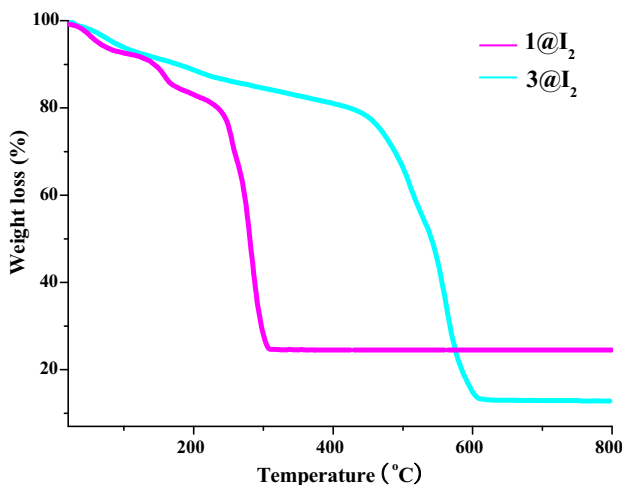


Fig. 8 TG curves of **1**@I₂ and **3**@I₂.

samples for **1** and **2** are also measured. Also as shown in Fig. 7, for each, it is the same as that of the corresponding title compound, implying that the host framework does not change after the release of I₂.

The kinetics of the I₂ release processes for **1** and **3** were investigated. To a 3.5 mL ethanol-containing colorimeter cell, 1 mg **1**@I₂ or **3**@I₂ was added. The UV-Vis spectrum is employed to monitor the I₂ concentration in the ethanol solution (see Fig. 10). The measured time interval is 6 min. Fig. 11

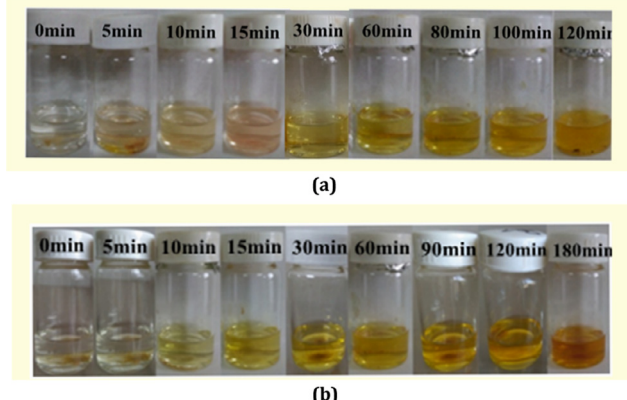


Fig. 9 Images showing I₂ release process for **1** (a) and **3** (b).

shows the time *vs* I₂ concentration curves for **1** and **3**. For the curve of **3**, in the initial 6 min, the slope of the curve is largest, indicating that in this stage, the rate of the I₂ release is the fastest. In the time range of 6–102 min, the curve is linear, suggesting that in this state, I₂ is released in a constant speed. After 102 min, the curve is almost horizontal, implying that the I₂ release has been close to a dynamic balance. Based on the time *vs* I₂ concentration curve of **1**, we can know that (i) in the beginning, the I₂ release is fastest. But the speed is slower than that of **3**; (ii) in the time range of 6–84 min, the speed is unstable; (iii) after 84 min, the speed turns slower; (iv) about

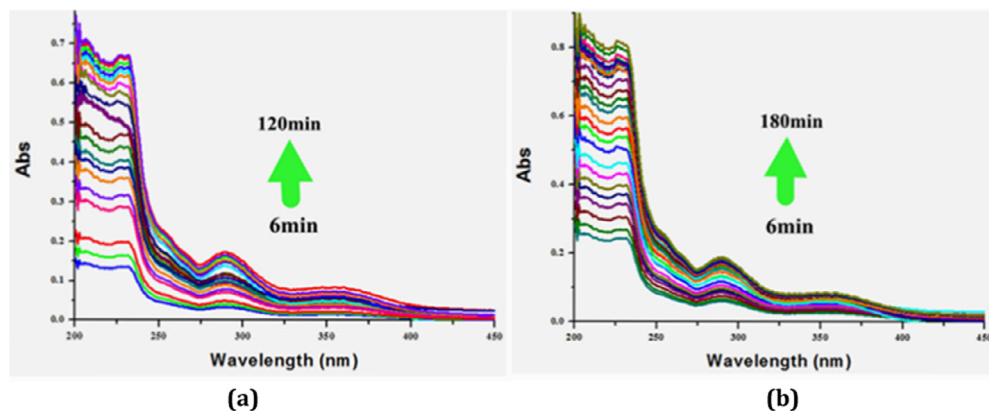


Fig. 10 UV-Vis spectra of **1** (a) and **3** (b), showing I_2 release process.

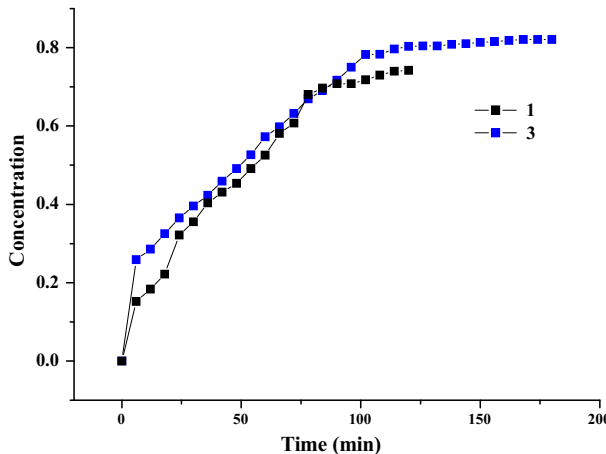


Fig. 11 Time vs I_2 concentration curves for **1** and **3**.

108 min, the speed is close to zero, indicating that the I_2 release is in a balance state.

Just as expected, both **1** and **3** can adsorb the I_2 molecule, and the adsorption is reversible. Even though the voids in the structure of **3** (978 \AA^3) is slightly smaller than that in **1** (1055 \AA^3), the adsorption capacity of **3** is a bit stronger than that of **1**. Especially, **3** can quickly adsorb the I_2 molecule. Only about 5 s, the adsorption is close to a balance. This should be related to the number and the distribution for the uncoordinated N/O atoms on the side walls of the channels. In H_3L2 , there are twelve potential donor atoms. But in **3**, only three N atoms participate in the coordination with the metal center, while the other nine atoms are uncoordinated. These nine atoms are distributed on the side walls of the channels, and most O atoms protrude from the walls (see Fig. 2c). These protruded O atoms can induce the I_2 molecules to quickly enter the channels via the weak O/O-H \cdots I interactions. While the other donor atoms can aid these protruded O atoms to hold the I_2 molecules, making them stay at the channels. For H_2L1 in **1**, only three N/O atoms are uncoordinated, and one O atom protrudes to the outside of the tube (see Fig. 1d). These structural factors will directly affect the adsorption property of the material including the capacity and the speed. Moreover, a reasonable arrangement for the adsorbed I_2 molecule in the channels

can improve the adsorption capacity of the material. On the contrary, an irrational distribution will impede the continuous entrance of the I_2 molecules. Those weak interactions should control the arrangement of the adsorbed I_2 molecule in the channels, since they possess the directivity.

4. Conclusion

In summary, we reported the synthesis, structure, and the reversible I_2 adsorption property of three new porous acylhydrazide-based Zn^{2+}/Cd^{2+} coordination polymers. The acylhydrazide molecules originated from the *in situ* acylation of the corresponding acids with N_2H_4 . **3** is the first example of triacylhydrazide-based coordination polymer. Synthetically, the pH level, temperature, and the amount of N_2H_4 play a key role in the reactions. Structurally, the porous formation should be related to the four factors: (i) the configuration of the ligand node; (ii) the tetrahedral configuration of the metal center; (iii) the distance between the acylhydrazide group and the other donor atoms; (iv) the rigidity of the ligand. The investigation on the I_2 adsorption property for two Zn^{2+} compounds reveals that both can reversibly adsorb the I_2 molecule. Although the pore in **3** is smaller than that in **1**, (i) the adsorption capacity of **3** is a bit stronger than that of **1**; (ii) **3** can quickly adsorb I_2 . These should be related to the number and the distribution for the uncoordinated N/O atoms on the side walls of the channels: (i) the protruded atoms can induce I_2 to quickly enter the channels; (ii) the other atoms can aid the protruded atoms to hold I_2 ; (iii) these atoms can also control the arrangement of I_2 within the channels via the weak N/O \cdots I interactions.

Acknowledgements

This research was supported by the National Natural Science Foundation of China (no. 21771076).

Appendix A. Supplementary material

Supplementary data associated with this article can be found, in the online version, at <https://doi.org/10.1016/j.arabjc.2018.07.004>.

References

- Ahmad, W., Zhang, L., Zhou, Y., 2014a. *CrystEngComm* 16, 3521–3531.
- Ahmad, W., Zhang, L., Zhou, Y., 2014b. *Photochem. Photobiol. Sci.* 13, 660–670.
- Ahmad, W., Zhang, L., Zhou, Y., 2014c. *Photochem. Photobiol. Sci.* 13, 660–670.
- Ahmed, E., Rothenberger, A., 2016a. *Micropor. Mesopor. Mater.* 220, 247–252.
- Ahmed, E., Rothenberger, A., 2016b. *Micropor. Mesopor. Mater.* 220, 247–252.
- Al-Maythalony, B.A., Shekhah, O., Swaidan, R., Belmabkhout, Y., Eddaoudi, I.P.M., 2015a. *J. Am. Chem. Soc.* 137, 1754–1757.
- Al-Maythalony, B.A., Shekhah, O., Swaidan, R., Belmabkhout, Y., Eddaoudi, I.P.M., 2015b. *J. Am. Chem. Soc.* 137, 1754–1757.
- Blanita, G., Mihet, M., Borodi, G., Misan, I., Coldea, I., Lupu, D., 2015. *Micropor. Mesopor. Mater.* 203, 195–201.
- Brunet, G., Safin, D.A., Aghajani, M.Z., Robeyns, K., Korobkov, I., Woo, T.K., Murugesu, M., 2017. *Chem. Sci.* 8, 3171–3177.
- Cao, L.H., Shi, F., Zhang, W.M., Zang, S.Q., Mak, T.C.W., 2015a. *Chem. Eur. J.* 21, 15705–15712.
- Cao, L.H., Shi, F., Zhang, W.M., Zang, S.Q., Mak, T.C.W., 2015b. *Chem. Eur. J.* 21, 15705–15712.
- Cao, L.H., Shi, F., Zhang, W.M., Zang, S.Q., Mak, T.C.W., 2015c. *Chem. Eur. J.* 21, 15705–15712.
- Chaemchuen, S., Zhou, K., Kabir, N.A., Chen, Y., Ke, X., Tendeloo, G.V., Verpoort, F., 2015. *Micropor. Mesopor. Mater.* 201, 277–285.
- Chen, Z., Adil, K., Weseliński, Ł.J., Belmabkhout, Y., Eddaoudi, M., 2015a. *J. Mater. Chem. A* 3, 6276–6281.
- Chen, Z., Adil, K., Weseliński, Ł.J., Belmabkhout, Y., Eddaoudi, M., 2015b. *J. Mater. Chem. A* 3, 6276–6281.
- Chen, Y.Z., Wang, C., Wu, Z.Y., Xiong, Y., Xu, Q., Yu, S.H., Jiang, H.L., 2015c. *Adv. Mater.* 27, 5010–5016.
- Chen, Y.Z., Wang, C., Wu, Z.Y., Xiong, Y., Xu, Q., Yu, S.H., Jiang, H.L., 2015d. *Adv. Mater.* 27, 5010–5016.
- Chen, Y.Z., Jiang, H.L., 2016a. *Chem. Mater.* 28, 6698–6704.
- Chen, Y.Z., Jiang, H.L., 2016b. *Chem. Mater.* 28, 6698–6704.
- Cui, Y., Song, T., Yu, J., Yang, Y., Wang, Z., Qian, G., 2015a. *Adv. Funct. Mater.* 25, 4796–4802.
- Cui, Y., Song, R., Yu, J., Liu, M., Wang, Z., Wu, C., Yang, Y., Wang, Z., Chen, B., Qian, G., 2015b. *Adv. Mater.* 27, 1420–1425.
- Cui, Y., Song, R., Yu, J., Liu, M., Wang, Z., Wu, C., Yang, Y., Wang, Z., Chen, B., Qian, G., 2015c. *Adv. Mater.* 27, 1420–1425.
- Cui, Y., Song, T., Yu, J., Yang, Y., Wang, Z., Qian, G., 2015d. *Adv. Funct. Mater.* 25, 4796–4802.
- Cui, Y., Li, B., He, H., Zhou, W., Chen, B., Qian, G., 2016a. *Acc. Chem. Res.* 49, 483–493.
- Cui, Y., Li, B., He, H., Zhou, W., Chen, B., Qian, G., 2016b. *Acc. Chem. Res.* 49, 483–493.
- Desai, A.V., Samanta, P., Manna, B., Ghosh, S.K., 2015a. *Chem. Commun.* 51, 6111–6114.
- Desai, A.V., Samanta, P., Manna, B., Ghosh, S.K., 2015b. *Chem. Commun.* 51, 6111–6114.
- Du, X., Fan, R., Fan, J., Qiang, L., Song, Y., Dong, Y., Xing, K., Wang, P., Yang, Y., 2016a. *Inorg. Chem. Front.* 3, 1480–1490.
- Du, X., Fan, R., Fan, J., Qiang, L., Song, Y., Dong, Y., Xing, K., Wang, P., Yang, Y., 2016b. *Inorg. Chem. Front.* 3, 1480–1490.
- Du, P.Y., Li, H., Fu, X., Gu, W., Liu, X., 2015. *Dalton Trans.* 44, 13752–13759.
- Fan, T.T., Li, J.J., Qu, X.L., Han, H.L., Li, X., 2015a. *CrystEngComm* 17, 9443–9451.
- Fan, T.T., Li, J.J., Qu, X.L., Han, H.L., Li, X., 2015b. *CrystEngComm* 17, 9443–9451.
- Fang, Z., Bueken, B., Vos, D.E.D., Fischer, R.A., 2015a. *Angew. Chem. Int. Ed.* 54, 7234–7254.
- Gabriel, C., Vangelis, A.A., Raptoptoulou, C.P., Terzis, A., Psycharis, V., Zervou, M., Bertmer, M., Salifoglou, A., 2015a. *Cryst. Growth Des.* 15, 5310–5326.
- Gabriel, C., Vangelis, A.A., Raptoptoulou, C.P., Terzis, A., Psycharis, V., Zervou, M., Bertmer, M., Salifoglou, A., 2015b. *Cryst. Growth Des.* 15, 5310–5326.
- Gao, M.L., Wang, W.J., Liu, L., Han, Z.B., Wei, N., Cao, X.M., Yuan, D.Q., 2017a. *Inorg. Chem.* 56, 511–517.
- Gao, M.L., Wang, W.J., Liu, L., Han, Z.B., Wei, N., Cao, X.M., Yuan, D.Q., 2017b. *Inorg. Chem.* 56, 511–517.
- Gao, W.Y., Wu, H., Leng, K., Sun, Y., Ma, S., 2016a. *Angew. Chem. Int. Ed.* 55, 5472–5476.
- Gao, W.Y., Wu, H., Leng, K., Sun, Y., Ma, S., 2016b. *Angew. Chem. Int. Ed.* 55, 5472–5476.
- Gao, Q., Xu, J., Cao, D., Chang, Z., Bu, X.H., 2016c. *Angew. Chem. Int. Ed.* 55, 15027–15030.
- Gao, Q., Xu, J., Cao, D., Chang, Z., Bu, X.H., 2016d. *Angew. Chem. Int. Ed.* 55, 15027–15030.
- Garai, M., Biradha, K., 2017. *Chem. Eur. J.* 23, 273–277.
- Gelfand, B.S., Huynh, R.P.S., Mah, R.K., Shimizu, G.K.H., 2016a. *Angew. Chem. Int. Ed.* 55, 14614–14617.
- Gelfand, B.S., Huynh, R.P.S., Mah, R.K., Shimizu, G.K.H., 2016b. *Angew. Chem. Int. Ed.* 55, 14614–14617.
- Gygi, D., Bloch, E.D., Mason, J.A., Hudson, M.R., Gonzalez, M.I., Siegelman, R.L., Darwish, T.A., Queen, W.L., Brown, C.M., Long, J.R., 2016a. *Chem. Mater.* 28, 1128–1138.
- Gygi, D., Bloch, E.D., Mason, J.A., Hudson, M.R., Gonzalez, M.I., Siegelman, R.L., Darwish, T.A., Queen, W.L., Brown, C.M., Long, J.R., 2016b. *Chem. Mater.* 28, 1128–1138.
- Herzberger, J., Niederer, K., Pohlit, H., Seiwert, J., Worm, M., Wurm, F.R., Frey, H., 2016. *Chem. Rev.* 116, 2170–2243.
- Hong, W.Y., Perera, S.P., Burrows, A.D., 2015. *Micropor. Mesopor. Mater.* 214, 149–155.
- Hu, K.Q., Jiang, X., Wang, C.Z., Mei, L., Xie, Z.N., Tao, W.Q., Zhang, X.L., Chai, Z.F., Shi, W.Q., 2017a. *Chem. Eur. J.* 23, 529–532.
- Hu, K.Q., Jiang, X., Wang, C.Z., Mei, L., Xie, Z.N., Tao, W.Q., Zhang, X.L., Chai, Z.F., Shi, W.Q., 2017b. *Chem. Eur. J.* 23, 529–532.
- Huang, L., He, M., Chen, B., Hu, B., 2015a. *J. Mater. Chem. A* 3, 11587–11595.
- Huang, L., He, M., Chen, B., Hu, B., 2015b. *J. Mater. Chem. A* 3, 11587–11595.
- Huang, J.J., Zhang, X., Huo, Q.S., Yu, J.H., Xu, J.Q., 2016. *Inorg. Chem. Front.* 3, 406–416.
- Jiao, J., Liu, H., Chen, F., Bai, D., Xiong, S., He, Y., 2016. *Inorg. Chem. Front.* 3, 1411–1418.
- Karmakar, A., Martins, L.M.D.R.S., Hazra, S., Silva, M.F.C.G., Pombeiro, A.J.L., 2016. *Cryst. Growth Des.* 16, 1837–1849.
- Krause, S., Bon, V., Senkovska, I., Stoeck, U., Wallacher, D., Többens, D.M., Zander, S., Pillai, R.S., Maurin, G., Coudert, F.X., Kaskel, S., 2016a. *Nature* 532, 348–352.
- Krause, S., Bon, V., Senkovska, I., Stoeck, U., Wallacher, D., Többens, D.M., Zander, S., Pillai, R.S., Maurin, G., Coudert, F.X., Kaskel, S., 2016b. *Nature* 532, 348–352.
- Lee, S., Kapustin, E.A., Yaghi, O.M., 2016a. *Science* 353 (353), 808–811.
- Lee, S., Kapustin, E.A., Yaghi, O.M., 2016b. *Science* 353 (353), 808–811.
- Levine, D.J., Runčevski, T., Kapelewski, M.T., Keitz, B.K., Oktawiec, J., Reed, D.A., Mason, J.A., Jiang, H.Z.H., Colwell, K.A., Legendre, C.M., FitzGerald, S.A., Long, J.R., 2016a. *J. Am. Chem. Soc.* 138, 10143–10150.
- Levine, D.J., Runčevski, T., Kapelewski, M.T., Keitz, B.K., Oktawiec, J., Reed, D.A., Mason, J.A., Jiang, H.Z.H., Colwell, K.A.,

- Legendre, FitzGerald, S.A., Long, J.R., . *J. Am. Chem. Soc.* 138, 10143–10150.
- Levine, D.J., Runčevski, T., Kapelewski, M.T., Keitz, B.K., Oktawiec, J., Reed, D.A., Mason, J.A., Jiang, H.Z.H., Colwell, K.A., Legendre, C.M., FitzGerald, S.A., Long, J.R., 2016c. *J. Am. Chem. Soc.* 138, 10143–10150.
- Levine, D.J., Runčevski, T., Kapelewski, M.T., Keitz, B.K., Oktawiec, J., Reed, D.A., Mason, J.A., Jiang, H.Z.H., Colwell, K.A., Legendre, C.M., FitzGerald, S.A., Long, J.R., 2016d. *J. Am. Chem. Soc.* 138, 10143–10150.
- Li, J.J., Fan, T.T., Qu, X.L., Han, H.L., Li, X., 2016a. *Dalton Trans.* 45, 2924–2935.
- Li, J.J., Fan, T.T., Qu, X.L., Han, H.L., Li, X., 2016b. *Dalton Trans.* 45, 2924–2935.
- Li, H., Hill, M.R., Huang, R., Doblin, C., Lim, S., Hill, A.J., Babarao, R., Falcaro, P., 2016c. *Chem. Commun.* 52, 5973–5976.
- Li, H., Hill, M.R., Huang, R., Doblin, C., Lim, S., Hill, A.J., Babarao, R., Falcaro, P., 2016d. *Chem. Commun.* 52, 5973–5976.
- Li, J.R., Kuppler, R.J., Zhou, H.C., 2009a. *Chem. Soc. Rev.* 38, 1477–1504.
- Li, J.R., Kuppler, R.J., Zhou, H.C., 2009b. *Chem. Soc. Rev.* 38, 1477–1504.
- Li, P.Z., Wang, X.J., Tan, S.Y., Ang, C.Y., Chen, H., Liu, J., Zou, R., Zhao, Y., 2015a. *Angew. Chem. Int. Ed.* 54, 12748–12752.
- Li, P.Z., Wang, X.J., Tan, S.Y., Ang, C.Y., Chen, H., Liu, J., Zou, R., Zhao, Y., 2015b. *Angew. Chem. Int. Ed.* 54, 12748–12752.
- Lin, Y., Kong, C., Zhang, Q., Chen, L., 2017a. *Adv. Energy Mater.* 7, 1601296.
- Lin, Y., Kong, C., Zhang, Q., Chen, L., 2017b. *Adv. Energy Mater.* 7, 1601296.
- Lin, J.X., Liang, J., Feng, J.F., Karadeniz, B., Lü, J., Cao, R., 2016a. *Inorg. Chem. Front.* 3, 1393–1397.
- Lin, J.X., Liang, J., Feng, J.F., Karadeniz, B., Lü, J., Cao, R., 2016b. *Inorg. Chem. Front.* 3, 1393–1397.
- Lucier, B.E.G., Zhang, Y., Lee, K.J., Lu, Y., Huang, Y., 2016a. *Chem. Commun.* 52, 7541–7544.
- Lucier, B.E.G., Zhang, Y., Lee, K.J., Lu, Y., Huang, Y., 2016b. *Chem. Commun.* 52, 7541–7544.
- Luo, X.P., Fu, S.Y., Du, Y.M., Guo, J.Z., Li, B., 2017a. *Micropor. Mesopor. Mater.* 237, 268–274.
- Luo, X.P., Fu, S.Y., Du, Y.M., Guo, J.Z., Li, B., 2017b. *Micropor. Mesopor. Mater.* 237, 268–274.
- Luo, F., Lin, Y., Zheng, L., Lin, X., Chi, Y., *Appl. A.C.S.*, 2015. *Mater. Inter.* 7, 11322–11329.
- Ma, H.F., Liu, Q.Y., Wang, Y.L., Yin, S.G., 2017a. *Inorg. Chem.* 56, 2919–2925.
- Ma, H.F., Liu, Q.Y., Wang, Y.L., Yin, S.G., 2017b. *Inorg. Chem.* 56, 2919–2925.
- Ma, J., Ying, Y., Guo, X., Huang, H., Liu, D., Zhong, C., 2016a. *J. Mater. Chem. A* 4, 7281–7288.
- Ma, J., Ying, Y., Guo, X., Huang, H., Liu, D., Zhong, C., 2016b. *J. Mater. Chem. A* 4, 7281–7288.
- Maiti, S., Pramanik, A., Manju, U., Mahanty, S., 2016a. *Micropor. Mesopor. Mater.* 226, 353–359.
- Maiti, S., Pramanik, A., Manju, U., Mahanty, S., 2016b. *Micropor. Mesopor. Mater.* 226, 353–359.
- Manna, K., Zhang, T., Greene, F.X., Lin, W., 2015a. *J. Am. Chem. Soc.* 137, 2665–2673.
- Manna, K., Zhang, T., Greene, F.X., Lin, W., 2015b. *J. Am. Chem. Soc.* 137, 2665–2673.
- Morzyk-Ociepa, B., 2007a. *J. Mol. Struct.* 846, 74–86.
- Morzyk-Ociepa, B., 2007b. *J. Mol. Struct.* 833, 121–132.
- Morzyk-Ociepa, B., 2007c. *J. Mol. Struct.* 833, 121–132.
- Morzyk-Ociepa, B., 2007d. *J. Mol. Struct.* 846, 74–86.
- Nandi, S., Collins, S., Chakraborty, D., Banerjee, D., Thallapally, P., Woo, T.K., Vaidhyanathan, R., 2017a. *J. Am. Chem. Soc.* 139, 1734–1737.
- Nandi, S., Collins, S., Chakraborty, D., Banerjee, D., Thallapally, P., Woo, T.K., Vaidhyanathan, R., 2017b. *J. Am. Chem. Soc.* 139, 1734–1737.
- Parshamoni, S., Telangae, J., Sanda, S., Konar, S., 2016. *Chem. Asian J.* 11, 540–547.
- Rosnes, M.H., Opitz, M., Frontzek, M., Lohstroh, W., Embs, J.P., Georgiev, P.A., Dietzel, P.D.C., 2015a. *J. Mater. Chem. A* 3, 4827–4839.
- Rosnes, M.H., Opitz, M., Frontzek, M., Lohstroh, W., Embs, J.P., Georgiev, P.A., Dietzel, P.D.C., 2015b. *J. Mater. Chem. A* 3, 4827–4839.
- Sheldrick, G.M., 2008. *Acta Crystallogr Sect. A: Fundam. Crystallogr.* A 64, 112–122.
- Shi, D., He, C., Qi, B., Chen, C., Niu, J., Duan, C., 2015a. *Chem. Sci.* 6, 1035–1042.
- Shi, D., He, C., Qi, B., Chen, C., Niu, J., Duan, C., 2015b. *Chem. Sci.* 6, 1035–1042.
- Sikdar, N., Bonakala, S., Haldar, R., Balasubramanian, S., Maji, T., 2016a. *Chem. Eur. J.* 22, 6059–6070.
- Sikdar, N., Bonakala, S., Haldar, R., Balasubramanian, S., Maji, T., 2016b. *Chem. Eur. J.* 22, 6059–6070.
- Tang, Y., He, C., Mitchell, L.A., Parrish, D.A., Shreeve, J.M., 2016. *Angew. Chem. Int. Ed.* 55, 5565–5567.
- Ugale, B., Dhankhar, S.S., Nagaraja, C.M., 2016a. *Inorg. Chem.* 55, 9757–9766.
- Ugale, B., Dhankhar, S.S., Nagaraja, C.M., 2016b. *Inorg. Chem.* 55, 9757–9766.
- Wang, Y.N., Bai, F.Q., Yu, J.H., Xu, J.Q., 2013a. *Dalton Trans.* 42, 16547–16555.
- Wang, Y.N., Bai, F.Q., Yu, J.H., Xu, J.Q., 2013b. *Dalton Trans.* 42, 16547–16555.
- Wang, H., Qin, J., Huang, C., Han, Y., Xu, W., Hou, H., 2016a. *Dalton Trans.* 45, 12710–12716.
- Wang, H., Qin, J., Huang, C., Han, Y., Xu, W., Hou, H., 2016b. *Dalton Trans.* 45, 12710–12716.
- Wang, H., Cheng, F., Zou, C., Li, Q., Hua, Y., Duan, J., Jin, W., 2016c. *CrystEngComm* 18, 5639–5646.
- Wang, H., Cheng, F., Zou, C., Li, Q., Hua, Y., Duan, J., Jin, W., 2016d. *CrystEngComm* 18, 5639–5646.
- Wang, Z., Li, X.Y., Liu, L.W., Yu, S.Q., Feng, Z.Y., Tung, C.H., Sun, D., 2016e. *Chem. Eur. J.* 22, 6830–6836.
- Wang, Z., Li, X.Y., Liu, L.W., Yu, S.Q., Feng, Z.Y., Tung, C.H., Sun, D., 2016f. *Chem. Eur. J.* 22, 6830–6836.
- Wang, B., Lv, X.L., Feng, D., Xie, L.H., Zhang, J., Li, M., Xie, Y., Li, J.R., Zhou, H.C., 2016g. *J. Am. Chem. Soc.* 138, 6204–6216.
- Wang, B., Lv, X.L., Feng, D., Xie, L.H., Zhang, J., Li, M., Xie, Y., Li, J.R., Zhou, H.C., 2016h. *J. Am. Chem. Soc.* 138, 6204–6216.
- Wang, Y.N., Huo, Q.S., Zhang, P., Yu, J.H., Xu, J.Q., 2016i. *Spectrochim. Acta A* 167, 33–40.
- Wang, D., Zhou, J., Chen, R., Shi, R., Zhao, G., Xia, G., Li, R., Liu, Z., Tian, J., Wang, H., Guo, Z., Wang, H., 2016j. *Biomaterials* 100, 27–40.
- Wang, Y.N., Li, G.H., Yang, Q.F., Yu, J.H., Xu, J.Q., 2014a. *CrystEngComm* 16, 2692–2701.
- Wang, Y.N., Yang, Q.F., Li, G.H., Zhang, P., Yu, J.H., Xu, J.Q., 2014b. *Dalton Trans.* 43, 11646–11657.
- Wang, Y.N., Yu, J.H., Xu, J.Q., 2014c. *Inorg. Chem. Front.* 1, 673–681.
- Wang, Y.N., Yu, J.H., Xu, J.Q., 2014d. *Polyhedron* 83, 220–227.
- Wang, Y.N., Li, G.H., Bai, F.Q., Yu, J.H., Xu, J.Q., 2014e. *Dalton Trans.* 43, 15617–15627.
- Wang, Y.N., Yang, Q.F., Li, G.H., Zhang, P., Yu, J.H., Xu, J.Q., 2014f. *Dalton Trans.* 43, 11646–11657.
- Wang, Y.N., Yu, J.H., Xu, J.Q., 2014g. *Polyhedron* 83, 220–227.
- Wang, Y.N., Zhang, P., Yu, J.H., Xu, J.Q., 2015a. *Dalton Trans.* 44, 1655–1663.
- Wang, Y.N., Zhang, P., Yu, J.H., Xu, J.Q., 2015b. *Dalton Trans.* 44, 1655–1663.

- Wang, Y.N., Yu, J.H., Xu, J.Q., 2015c. *ChemPlusChem.* 80, 1732–1740.
- Wang, Y.N., Yang, Q.F., Huo, Q.S., Yu, J.H., Xu, J.Q., 2017. *Polyhedron* 130, 154–159.
- Whitcomb, D.R., Rajeswaran, M., 2006a. *J. Chem. Crystallogr.* 36, 587–598.
- Whitcomb, D.R., Rajeswaran, M., 2006b. *J. Chem. Crystallogr.* 36, 587–598.
- Xie, W., He, W.W., Li, S.L., Shao, K.Z., Su, Z.M., Lan, Y.Q., 2016a. *Chem. Eur. J.* 22, 17298–17304.
- Xie, W., He, W.W., Li, S.L., Shao, K.Z., Su, Z.M., Lan, Y.Q., 2016b. *Chem. Eur. J.* 22, 17298–17304.
- Xie, W., Qin, J.S., He, W.W., Shao, K.Z., Su, Z.M., Du, D.Y., Li, S.L., Lan, Y.Q., 2017. *Inorg. Chem. Front.* 4, 547–552.
- Xu, X.Y., Yan, B., Appl, A.C.S., 2015. *Mater. Inter.* 7, 721–729.
- Xue, D.X., Belmabkhout, Y., Shekhhah, O., Jiang, H., Adil, K., Cairns, A.J., Eddaoudi, M., 2015a. *J. Am. Chem. Soc.* 137, 5034–5040.
- Xue, D.X., Belmabkhout, Y., Shekhhah, O., Jiang, H., Adil, K., Cairns, A.J., Eddaoudi, M., 2015b. *J. Am. Chem. Soc.* 137, 5034–5040.
- Yao, R.X., Cui, X., Jia, X.X., Zhang, F.Q., Zhang, X.M., 2016a. *Inorg. Chem.* 55, 9270–9275.
- Yao, R.X., Cui, X., Jia, X.X., Zhang, F.Q., Zhang, X.M., 2016b. *Inorg. Chem.* 55, 9270–9275.
- Yao, S., Xu, T., Zhao, N., Zhang, L., Huo, Q., Liu, Y., 2017. *Dalton Trans.* 46, 3332–3337.
- Ye, J.W., Zhou, H.L., Liu, S.Y., Cheng, X.N., Lin, R.B., Qi, X.L., Zhang, J.P., Chen, X.M., 2015a. *Chem. Mater.* 27, 8255–8260.
- Ye, J.W., Zhou, H.L., Liu, S.Y., Cheng, X.N., Lin, R.B., Qi, X.L., Zhang, J.P., Chen, X.M., 2015b. *Chem. Mater.* 27, 8255–8260.
- Yi, F.Y., Chen, D., Wu, M.K., Han, L., Jiang, H.L., 2016a. *ChemPlusChem.* 81, 675–690.
- Yi, F.Y., Chen, D., Wu, M.K., Han, L., Jiang, H.L., 2016b. *ChemPlusChem.* 81, 675–690.
- Yu, P., Li, Q., Hu, Y., Liu, N., Zhang, L., Su, K., Qian, J., Huang, S., Hong, M., 2016a. *Chem. Commun.* 52, 7978–7981.
- Yu, P., Li, Q., Hu, Y., Liu, N., Zhang, L., Su, K., Qian, J., Huang, S., Hong, M., 2016b. *Chem. Commun.* 52, 7978–7981.
- Yu, J.H., Zhu, Y.C., Wu, D., Yu, Y., Hou, Q., Xu, J.Q., 2009a. *Dalton Trans.*, 8248–8256.
- Yu, J.H., Zhu, Y.C., Wu, D., Yu, Y., Hou, Q., Xu, J.Q., 2009b. *Dalton Trans.*, 8248–8256.
- Yuan, B., Wang, J., Chen, Y., Wu, X., Luo, H., Deng, S., 2016a. *J. Mater. Chem. A* 4, 2263–2276.
- Yuan, B., Wang, J., Chen, Y., Wu, X., Luo, H., Deng, S., 2016b. *J. Mater. Chem. A* 4, 2263–2276.
- Zanchetta, E., Malfatti, L., Ricco, R., Styles, M.J., Lisi, F., Coghlan, C.J., Doonan, C.J., Hill, A.J., Brusatin, G., Falcaro, P., 2015a. *Chem. Mater.* 27, 690–699.
- Zanchetta, E., Malfatti, L., Ricco, R., Styles, M.J., Lisi, F., Coghlan, C.J., Doonan, C.J., Hill, A.J., Brusatin, G., Falcaro, P., 2015b. *Chem. Mater.* 27, 690–699.
- Zhang, J., Du, Y., Dong, K., Su, H., Zhang, S., Li, S., Pang, S., 2016a. *Chem. Mater.* 28, 1472–1480.
- Zhang, J., Du, Y., Dong, K., Su, H., Zhang, S., Li, S., Pang, S., 2016b. *Chem. Mater.* 28, 1472–1480.
- Zhang, Y., Feng, X., Yuan, S., Zhou, J., Wang, B., 2016c. *Inorg. Chem. Front.* 3, 896–909.
- Zhang, Y., Feng, X., Yuan, S., Zhou, J., Wang, B., 2016d. *Inorg. Chem. Front.* 3, 896–909.
- Zhang, Y., Yuan, S., Feng, X., Li, H., Zhou, J., Wang, B., 2016e. *J. Am. Chem. Soc.* 138, 5785–5788.
- Zhang, H., Zhang, M., Lin, P., Malgras, V., Tang, J., Alshehri, S.M., Yamauchi, Y., Du, S., Zhang, J., 2016f. *Chem. Eur. J.* 22, 1141–1145.
- Zhang, H., Zhang, M., Lin, P., Malgras, V., Tang, J., Alshehri, S.M., Yamauchi, Y., Du, S., Zhang, J., 2016g. *Chem. Eur. J.* 22, 1141–1145.
- Zhang, S.R., Li, J., Du, D.Y., Qin, J.S., Li, S.L., He, W.W., Su, Z.M., Lan, Y.Q., 2015a. *J. Mater. Chem. A* 3, 23426–23434.
- Zhang, S.R., Li, J., Du, D.Y., Qin, J.S., Li, S.L., He, W.W., Su, Z.M., Lan, Y.Q., 2015b. *J. Mater. Chem. A* 3, 23426–23434.
- Zhang, W.X., Liao, P.Q., Lin, R.B., Wei, Y.S., Zeng, M.H., 2015c. *Coord. Chem. Rev.* 293, 268–278.
- Zhang, W.X., Liao, P.Q., Lin, R.B., Wei, Y.S., Zeng, M.H., 2015d. *Coord. Chem. Rev.* 293, 268–278.
- Zhang, R.F., Shi, W., Wang, H.S., Cheng, P., 2008a. *J. Coord. Chem.* 61, 1606–1614.
- Zhang, R.F., Shi, W., Wang, H.S., Cheng, P., 2008b. *J. Coord. Chem.* 61, 1606–1614.
- Zhao, S.S., Chen, L., Zheng, X., Wang, L., Xie, Z., 2017. *Chem. Asian J.* 12, 615–620.
- Zhao, S.N., Song, X.Z., Zhu, M., Meng, X., Wu, L.L., Feng, J., Song, S.Y., Zhang, H.J., 2015a. *Chem. Eur. J.* 21, 9748–9752.
- Zhao, S.N., Song, X.Z., Zhu, M., Meng, X., Wu, L.L., Feng, J., Song, S.Y., Zhang, H.J., 2015b. *Chem. Eur. J.* 21, 9748–9752.
- Zhu, N.X., Zhao, C.W., Wang, J.C., Li, Y.A., Dong, Y.B., 2016. *Chem. Commun.* 52, 12702–12705.